2026 IEEE International Conference on Robotics and Automation (ICRA 2026)
June 1-5, 2026. Vienna, Austria

Connectivity Maintenance for High-Speed Communication With Adversarial Jamming

Thomas Kaminsky[1], Hammad Izhar[1], Daniel Garces[1], Collin Brady[2], Joseph Rottner[2], and Stephanie Gil[1]

***Abstract*— We consider the problem of adaptively controlling a fleet of robots to maintain a communication network in an adversarial environment. In particular, a *network team* of robots is tasked with maintaining a directed communication channel at some data rate γ from an independent *task robot* to a fixed *base station*, accommodating the task robot's motion and adversarial intervention in the form of an omnidirectional jammer and network team robot removals. We utilize a physically-motivated model for directed signal strength between robots in the presence of a jammer, introducing asymmetry into communication which challenges connectivity maintenance approaches [1]. Our main contribution in this paper is the introduction of a strategy for translating this directed model into an undirected graph for which enforcing connectedness is sufficient for maintaining high-rate communication. We demonstrate the efficacy of our approach in simulation using a CBF-based controller, showing that our controller maintains a high-rate connection throughout diverse trajectories, even when more conservative controllers fail.**

I. INTRODUCTION

Ad-hoc networks are critical for robust communication for applications such as search and rescue [2], [3], where a base station must maintain communication with a mobile task robot for scouting [4], [5], target localization [6], [7], or coverage [8], [9], [10]. A fleet of robots can support the mission by placing themselves in the environment and forming a network to support diverse, time-varying, and potentially asymmetric communication needs. For instance, remote teleoperation requires a task robot to stream video to a pilot at the base as it moves, requiring a high-rate "forward" communication path, but the base only needs to relay velocity commands to the task robot, requiring a lower rate on the "reverse" path. While prior work has addressed the connectivity problem, it has largely focused on symmetric formulations, treating the forward and backward link quality as equal. This yields controllers that cannot handle asymmetric disturbances such as jammers. In contrast, in this work we consider the problem of maintaining a prescribed data rate along directed channels in asymmetric communication environments. This is essential for reliable task reporting and control in real-world systems operating under jamming.

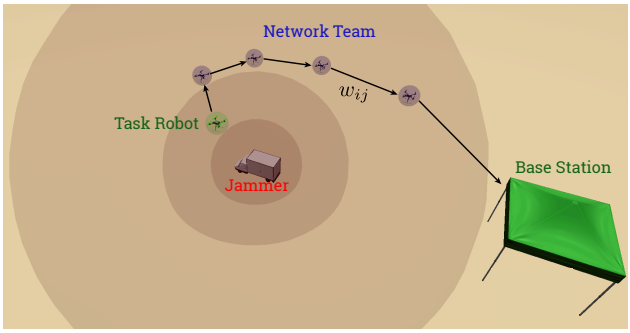

Fig. 1: Overview of problem setting. The network team (blue) supports a communication path from a task robot (green) to a base station (green) in the presence of a jammer (red). Each directed communication link has weight w_{ij}, related to the SINR.

Our work builds on *mobile infrastructure on demand* (MID) [11], [12], [13], [14], where a 'network team' of controllable robots support directed information flows—typically modeled via a desired minimum signal-to-noise ratio (SNR) or signal-to-interference-plus-noise ratio (SINR)—between members of a 'task team,' which follow arbitrary trajectories to accomplish some independent task. We focus on contested environments in which jammers can degrade communication quality by raising the noise floor for nearby receivers [15] and members of the network team can be adversarially removed without warning. These are central challenges for drone systems in the field [16], [17], [18], and are increasingly relevant for applications in urban environments such as delivery drones and emergency response [19], [20], [21].

Prior work models communication in two main ways. Learned or probabilistic models, such as neural networks [14], Gaussian processes [22] or stochastic decay functions [22], accurately capture channel uncertainty, but often lack performance guarantees since the communication landscape is stochastic or learned from data. Connectivity maintenance methods [1], [23], [24], [25], [26] instead model link quality as a non-negative function

[1]Thomas Kaminsky, Hammad Izhar, Daniel Garces, and Stephanie Gil are with the School of Engineering and Applied Sciences , Harvard University, Boston, MA 02134, United States tkaminsky@g.harvard.edu

[2]Collin Brady and Joseph Rottner are with MIT Lincoln Laboratory, Lexington, MA 02421, USA collin.brady@ll.mit.edu

DISTRIBUTION STATEMENT A. Approved for public release. Distribution is unlimited. This material is based upon work supported by the Under Secretary of War for Research and Engineering under Air Force Contract No. FA8702-15-D-0001 or FA8702-25-D-B-0002. Any opinions, findings, conclusions or recommendations expressed in this material are those of the author(s) and do not necessarily reflect the views of the Under Secretary of War for Research and Engineering. The authors gratefully acknowledge partial support through Lincoln Labs Line grant, AFOSR grant #FA9550-25-1-0140.

of inter-robot distances, which can be expressed as a weighted undirected graph. These approaches allow a network to ensure connectivity by using tools such as Control Barrier Functions (CBFs) [27] to enforce that the graph's Fiedler value remain positive while agents execute desired mission paths or controls [28], [1], [29], [30]. These approaches have achieved success in previous work due to their interpretability, strong theoretical guarantees, and flexibility in accommodating general control inputs.

Unfortunately, jammers introduce asymmetry into communication, since they impact the receiver but not the transmitter. This yields an asymmetric communication matrix, which cannot be controlled through the Fiedler value. Previous works considering jammed communication [31], [32] symmetrize the problem by considering the *minimum* between the two directed channels, but this results in a very conservative controller, since the asymmetric communication needs of each robot are not accounted for—for example, a teleoperated drone may still be able to transmit video back at a required rate through the forward channel while near a jammer, though the capacity of the reverse channel may be much weaker.

This asymmetry is thus the key gap: existing undirected frameworks cannot maintain high-rate directed channels in the presence of jammers without unnecessarily constraining the task robot's motion, since they must both be able to transmit and receive at a high rate. This motivates new methods that retain the simplicity and theoretical soundness of connectivity maintenance, while handling the asymmetry of communication that can arise naturally, as in contested environments.

In this work, we cast the problem of mobile infrastructure on demand for serial communication from a single source to a single sink in contested environments with adversarial jamming as a *modified* connectivity maintenance problem. In Section III-B, following previous work [31], we provide a communication model inspired by antenna theory [15] which realistically models the asymmetric effect of an omnidirectional jammer ((3)). To accommodate this asymmetry, in Section IV-A we introduce a special class of undirected graphs, which we call *symmetrized control graphs*, for which enforcing a positive Fiedler value is sufficient to guarantee a directed communication channel from the task robot to the base station with rate at least γ (Proposition IV.3). Analysis of this class of graphs forms the central contribution of our work.

In Section IV-B, we construct a CBF-based controller inspired by [1] to control the network team ((10)), and we verify that feasible solutions maintain communication at rate γ in the presence of an environmental jammer. Finally, in Section V we verify the efficacy of our approach in simulation, demonstrating that our controller both maintains a high-rate path and enables more ambitious task robot trajectories than a controller enforcing minimum channel strength.

II. BACKGROUND

A. Mathematical Preliminaries

We write scalar quantities in plain script (e.g. h, t), vectors with lowercase boldface (e.g. $\mathbf{x}, \mathbf{u}$) and matrices with capital boldface (e.g. $\mathbf{X}, \mathbf{W}$). Let $\mathbf{I}_N$ denote the identity matrix in $\mathbb{R}^{N\times N}$, and let $\mathbf{e}_i$ denote the i-th column of an identity matrix whose dimension is clear from context. Let $\mathbf{0}_{M\times N}$ (or $\mathbf{0}_M$, if $N = 1$) denote the matrix of all 0's in $\mathbb{R}^{M\times N}$, and likewise let $\mathbf{1}_{M\times N}$ (or $\mathbf{1}_N$) denote the vector of all 1's. Let $(f \circ g)(x) = f(g(x))$ denote the *composition* of f and g.

A *weighted directed graph* is given by a tuple $\mathcal{G} = (\mathcal{V}, \mathcal{E}, \mathbf{W})$, where $\mathcal{V}$ is a set of vertices, $\mathcal{E} \subseteq \{(i,k) \mid i,k \in \mathcal{V}\}$ is a set of directed edges between vertices, and $\mathbf{W} \in \mathbb{R}_{\geq 0}^{|\mathcal{V}|\times|\mathcal{V}|}$ is a weight matrix with entries $\mathbf{W}_{ik} > 0$ if $(i,k) \in \mathcal{E}$, and 0 otherwise. The following concepts will also be useful:

Definition II.1 (Path). Given a weighted directed graph $\mathcal{G} = (\mathcal{V}, \mathcal{E}, \mathbf{W})$, a *path* P from node v to node w is a sequence of distinct vertices $P = (i_1, \ldots, i_N)$ with the properties that $i_1 = v$, $i_N = w$, and $(i_k, i_{k+1}) \in \mathcal{E}$ for all $k < N$. We denote by $v \to w$ a generic directed path from v to w, and an undirected path by $v \text{ — } w$.

Definition II.2 (Vertex-Independence). Two paths are called *vertex-independent* if they share no vertices in common, except possibly their start and end points.

Definition II.3 (Path-Induced Subgraph). Given a set of paths $\mathcal{P}$, its *path-induced subgraph* $\mathcal{G}_\mathcal{P}$ is the graph constructed by taking each path's vertices $\mathcal{V}_\mathcal{P} = \bigcup_{P\in\mathcal{P}} \bigcup_{k=1}^{|P|} \{i_k\}$, associated edges $\mathcal{E}_\mathcal{P} = \bigcup_{P\in\mathcal{P}} \bigcup_{k=1}^{|P|-1} \{(i_k, i_{k+1})\}$, and edge weights $[\mathbf{W}_\mathcal{P}]_{vw} = \mathbf{W}_{vw}$ if $(v,w) \in \mathcal{E}_\mathcal{P}$, and 0 otherwise.

B. Control Barrier Functions

In order to ensure strong communication, we will enforce safety as a constraint using Control Barrier Functions (CBFs) [27]. The goal of a CBF is to enforce *forward invariance* of a dynamical system. That is, if a system evolves by some dynamics

$$\dot{\mathbf{x}}(t) = F(\mathbf{x}) + G(\mathbf{x})\mathbf{u}(\mathbf{x}), \tag{1}$$

then given a desired safe set $\mathcal{C}$, we seek to design a control input $\mathbf{u}(\mathbf{x}) \in U$ such that, if $\mathbf{x}(0) \in \mathcal{C}$, then $\mathbf{x}(t) \in \mathcal{C} \ \ \forall t \geq 0$. Intuitively, CBFs reduce the problem of set invariance to verifying a differential inequality at each timestep:

Definition II.4 (Control Barrier Function (CBF)). A continuously-differentiable function $h : \mathcal{D} \to \mathbb{R}$, where $\mathcal{D}$ is some set satisfying $\mathcal{C} \subseteq \mathcal{D} \subseteq \mathbb{R}^n$, is called a *control barrier function (CBF)* if there exists an extended class $\mathcal{K}_\infty$ function α such that, for the dynamics (1),

$$\sup_{\mathbf{u}\in U} \left[\frac{dh(x)}{dt}\right] \geq -\alpha(h(x)) \tag{2}$$

for all $x \in \mathcal{D}$. A function $\alpha : \mathbb{R} \to \mathbb{R}$ is called an **extended class $\mathcal{K}_\infty$ function** if α is strictly increasing and $\alpha(0) = 0$.

For such a function, we can design a safe controller if the following holds:

Theorem II.5 (Theorem 2 of [27])**.** If $\mathcal{C}$ is a 0-superlevel set of a control barrier function $h : \mathcal{D} \to \mathbb{R}$, and $\frac{\partial h}{\partial \mathbf{x}}(\mathbf{x}) \neq \mathbf{0}$ for all $\mathbf{x} \in \partial\mathcal{C}$, then any Lipschitz continuous controller $\mathbf{u}(\mathbf{x})$ which results in

$$\frac{\partial h(\mathbf{x})}{\partial t} \geq -\alpha(h(\mathbf{x}))$$

for all $\mathbf{x} \in \mathcal{C}$ is forward-invariant with respect to $\mathcal{C}$.

III. PROBLEM FORMULATION

We describe below the problem setting, attack model, and control objective.

A. Robots and Positions

We possess a network team composed of K robots whose positions at time t are denoted by $\mathbf{x}_1(t), \mathbf{x}_2(t), \ldots, \mathbf{x}_K(t) \in \mathbb{R}^2$. Likewise, we have a task robot T with position $\mathbf{x}_{\mathrm{T}}(t) \in \mathbb{R}^2$, and a static base station B with position $\mathbf{x}_{\mathrm{B}} \in \mathbb{R}^2$. We vectorize their positions as follows (so $\mathbf{X}(t) \in \mathbb{R}^{(K+2)\times 2}$):

$$\mathbf{X}(t) = \begin{bmatrix}\mathbf{x}_1(t) & \mathbf{x}_2(t) & \ldots & \mathbf{x}_K(t) & \mathbf{x}_{\mathrm{T}}(t) & \mathbf{x}_{\mathrm{B}}(t)\end{bmatrix}^\top.$$

Finally, we allow for the presence of an adversary in the form of a jammer J with known static position $\mathbf{x}_{\mathrm{J}} \in \mathbb{R}^2$. For brevity, we will often refer to the task robot as T, the base station as B, and the jammer as J.

B. Communication

To model the communication strength between two robots, we take inspiration from the Friis transmission model [15], with the jammer serving as an isotropic radiator that raises the noise floor for proximate robots. In particular, given a configuration of robots $\mathbf{X} = \begin{bmatrix}\mathbf{x}_1 & \mathbf{x}_2 & \ldots & \mathbf{x}_K & \mathbf{x}_{\mathrm{T}} & \mathbf{x}_{\mathrm{B}}\end{bmatrix}^\top$ and jammer position $\mathbf{x}_{\mathrm{J}}$, we define the *signal-to-interference-plus-noise ratio (SINR)* of the channel from robot i to robot k as

$$L_{ik}^{\text{SINR}}(\mathbf{X}) \triangleq \frac{C_S \left\|\mathbf{x}_i - \mathbf{x}_k\right\|^{-2}}{N_F + C_J \left\|\mathbf{x}_k - \mathbf{x}_J\right\|^{-2}},$$

where parameters $C_S, C_J > 0$ encode the power of the signal and jammer, respectively, and $N_F > 0$ encodes the noise floor of the environment. The SINR describes the power of the signal that $\mathbf{x}_k$ receives from $\mathbf{x}_i$, relative to noise intrinsic to the environment (the *noise floor* N_F) and noise due to interference (the *jammer power* $C_J||\mathbf{x}_k - \mathbf{x}_{\mathrm{J}}||^{-2}$). The SINR has been shown to correlate strongly with the highest achievable data rate for a given channel [33]. However, since the SINR diverges as $\mathbf{x}_i \to \mathbf{x}_k$, we instead work with an underapproximation of the SINR, which we call the *link quality* from i to k:

$$L_{ik}(\mathbf{X}) \triangleq \frac{C_S[\delta + \left\|\mathbf{x}_i - \mathbf{x}_k\right\|]^{-2}}{N_F + C_J \left\|\mathbf{x}_k - \mathbf{x}_J\right\|^{-2}}, \tag{3}$$

where $\delta > 0$ can be an arbitrary positive offset. Since $L_{ik} \leq L_{ik}^{\text{SINR}}$, guaranteeing high link quality ensures high SINR, while retaining the nice property of being a continuously-differentiable function on $\mathbb{R}^{(K+2)\times 2}$.

The goal of control is to maintain a high-rate connection from the task robot to the base station. Letting $\gamma > 0$ denote some minimum viable SINR, we formalize this notion as follows:

Definition III.1 (**γ-strong Path**)**.** We call an edge (i, k) *γ-strong* if $L_{ik} > \gamma$. Likewise, we call a path P γ-strong if (i_k, i_{k+1}) is γ-strong for each $k \in \{1, \ldots, |P| - 1\}$.

Then the objective of control is to maintain a γ-strong path from T $\to$ B. This is analogous to the problem of mobile infrastructure on demand ([13]), though we model the data rate using the highest achievable SINR along serial communication paths rather than probabilistically along parallelized information flows. It is worth noting too that, due to the asymmetry inherent in our communication model, existence of a γ-strong path from $i \to k$ does not imply that one exists from $k \to i$.

We will view the γ-strong edges among cooperative robots as a weighted directed graph $\mathcal{G}_\gamma(\mathbf{X})$, with vertices given by $\mathcal{V}_\gamma(\mathbf{X}) = \{1, \ldots, K, \mathrm{T}, \mathrm{B}\}$, edges corresponding to all γ-strong edges, and directed weights given by each link's margin above the required rate γ:

$$[\mathbf{W}_\gamma(\mathbf{X})]_{ik} = \begin{cases} L_{ik}(\mathbf{X}) - \gamma & \text{if } L_{ik}(\mathbf{X}) > \gamma \\ 0 & \text{otherwise.} \end{cases} \tag{4}$$

We call this graph the **γ-threshold graph** for a configuration of robots. By construction, this graph has a directed edge (i, j) if and only if that edge can transmit messages at rate at least γ.

We assume for simplicity that robots can communicate with a centralized server at the base station at a rate sufficient to share positions, velocities, and control commands. The threshold γ corresponds to much higher-rate communication needs than those needed to relay control information (e.g. video streaming).

C. Attack Model

In addition to a jammer degrading link quality ((3)), we account for adversarial intervention in the form of *F faults* in which members of the network team are removed at arbitrary points in the trajectory. In particular we assume that removed robots never reenter the network at a later time and cannot communicate for the remainder of the mission.

D. Control

We allow the task robot to be controlled independently of the network team to accomplish some task. As such, its state evolves by an independent dynamic:

$$\dot{\mathbf{x}}_{\mathrm{T}}(t) = V_{\mathrm{T}}(t). \tag{5}$$

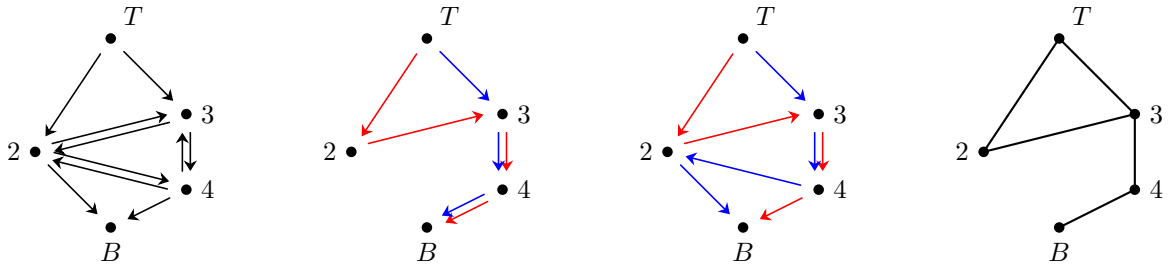

(a) (b) (c) (d)

Fig. 2: (a) An example γ-threshold graph $\mathcal{G}_\gamma$. (b) The induced subgraph of a path-consistent set $\mathcal{P}_1$. (c) The induced subgraph of a path-inconsistent set $\mathcal{P}_2$. (d) The symmetrized control graph $\mathcal{G}_C$ for $\mathcal{P}_1$.

The network team, on the other hand, can be controlled explicitly. Denote the control input for network robot i at time t as $\mathbf{u}_i(t) \in \mathbb{R}^2$. Then we assume single integrator dynamics with a feedback controller:

$$\dot{\mathbf{x}}_i(t) = \mathbf{u}_i(\mathbf{X}). \tag{6}$$

Stacking the control for the network team into a vector $\mathbf{u}(\mathbf{X}) = \begin{bmatrix} \mathbf{u}_1(\mathbf{X})^\top & \mathbf{u}_2(\mathbf{X})^\top & \dots & \mathbf{u}_K(\mathbf{X})^\top \end{bmatrix}^\top$, our dynamics can be vectorized as follows:

$$\dot{\mathbf{X}}(t) = \mathbf{e}_{2K+1} V_{\mathrm{T}}(t) + \begin{bmatrix} \mathbf{1}_{2K} \\ \mathbf{0}_2 \end{bmatrix} \mathbf{u}(\mathbf{X}).$$

IV. Analytical Results

Below, we describe our theoretical results. In Section IV-A, we introduce the concept of undirected *symmetrized control graphs*, which are derived from paths in the γ-threshold graph (Definition IV.2) and can be used to enforce strong communication using connectivity maintenance. In Section IV-B, we provide a CBF-based controller inspired by [1], whose feasible controls enforce that a symmetrized control graph remains connected, and thus contains a γ-strong path from $\mathrm{T} \to \mathrm{B}$.

A. Correspondence with Graph Properties

Consider the γ-threshold graph $\mathcal{G}_\gamma(\mathbf{X})$ for some configuration of robots. By construction, a γ-strong path exists from $\mathrm{T} \to \mathrm{B}$ if and only if there is a directed path from $\mathrm{T} \to \mathrm{B}$ in $\mathcal{G}_\gamma$. Likewise, the configuration is F-fault tolerant if and only if $\mathcal{G}_\gamma$ has $F+1$ vertex-independent paths from $\mathrm{T} \to \mathrm{B}$, by Menger's theorem [34]. Thus, we see that the γ-threshold graph exactly encodes both strong communication and F-fault tolerance. However, because $\mathcal{G}_\gamma$ is directed, it remains a challenge to control over this graph using the connectivity maintenance approaches of [28]. To address this, we propose a strategy for symmetrizing the γ-threshold graph so that connectedness of the resulting *symmetrized control graph* implies the existence of a γ-strong path from $\mathrm{T} \to \mathrm{B}$. The following notion is useful for constructing such graphs:

Definition IV.1 (Path Consistency). Let $\mathcal{P} = \{P_1, \dots, P_n\}$ be a set of paths from $\mathrm{T} \to \mathrm{B}$ with induced subgraph $\mathcal{G}_\mathcal{P}$. If there are no nodes $v, w \in \mathcal{G}_\mathcal{P}$, $v \neq w$ for which there simultaneously exist directed paths $\mathrm{T} \to v, w \to \mathrm{B}$, and $w \to v$, then we call the set $\mathcal{P}$ *path consistent*.

Path consistency ensures that no paths have 'reversed' links. For example, in Figure 2, the set in (b) is path consistent, but the set in (c) is not (e.g., nodes 2, 3). A consistent set of paths can form a *symmetrized control graph*:

Definition IV.2 (Symmetrized Control Graph). Given a path-consistent set $\mathcal{P}$, the undirected graph $\mathcal{G}_C$ constructed by treating each directed edge of $\mathcal{G}_\mathcal{P}$ as an undirected edge with weight $[\mathbf{W}_C]_{ik} = [\mathbf{W}_C]_{ki} = \mathbf{W}_{ik}$ is called a *symmetrized control graph*.

It is worth noting that constructing a symmetrized control graph requires choosing at most one directed edge between (i, k) and (k, i), as otherwise the undirected weight $[\mathbf{W}_C]_{ik}$ is ill-defined. We omit this condition, since path consistency implies that at most one of these directed edges is included in the set $\mathcal{P}$. Below, we show that the connectedness of such a graph $\mathcal{G}_C$ is sufficient for enforcing strong communication:

Proposition IV.3. Let $\mathcal{G}_C$ be any symmetrized control graph for a set of paths from $\mathrm{T} \to \mathrm{B}$ in $\mathcal{G}_\gamma$. If $\mathcal{G}_C$ is connected, then there exists a γ-strong path from $\mathrm{T} \to \mathrm{B}$.

Proof. Since $\mathcal{G}_C$ is connected and $\mathrm{T}, \mathrm{B} \in \mathcal{V}_C$ by construction, there must be an undirected path P from $\mathrm{T} \text{ — } \mathrm{B}$ in $\mathcal{G}_C$. Then assume towards contradiction that this path does not correspond to a proper directed path in $\mathcal{G}_\gamma$ from $\mathrm{T} \to \mathrm{B}$, meaning that one of the edges is facing in the wrong direction. Let $(i_k, i_{k+1}) \in P$ be the first such link; that is, the directed link in $\mathcal{G}_\mathcal{P}$ was (i_{k+1}, i_k). Then since $\mathcal{G}_C$ is generated by a set of paths from $\mathrm{T} \to \mathrm{B}$, there must exist a path P' from $i_{k+1} \to \mathrm{B}$ in $\mathcal{G}_\mathcal{P}$. But likewise, there is a directed path from $\mathrm{T} \to i_k$ by construction, as well as the one-edge path $i_{k+1} \to i_k$ given by the edge connecting them. But this contradicts path consistency (Definition IV.1) , so the link must face the right direction. Thus, a directed path $\mathrm{T} \to \mathrm{B}$ exists

in $\mathcal{G}_\gamma$, and so there exists a γ-strong path from T $\to$ B. $\square$

The same argument clearly holds for showing that $(F+1)$-connectivity (meaning there are at least $F+1$ vertex-disjoint paths from T $\to$ B) is sufficient for F-fault tolerance, by first subtracting any F robots. Moreover, we show that path consistency is tight, in the sense that any graph which violates path consistency must have a connected subgraph with no directed path from T $\to$ B:

Proposition IV.4. Let $\mathcal{G}_C$ be a graph constructed by the procedure in Definition IV.2, except that $\mathcal{P}$ is not path consistent. Then there exists a connected subgraph of $\mathcal{G}_C$ for which no undirected path from T — B corresponds to a proper directed path from T $\to$ B in $\mathcal{G}_\mathcal{P}$.

Proof. Let v, w be nodes violating path consistency, so there exist paths P_1 from T $\to v$, P_2 from $w \to$ B, and P_3 from $w \to v$. We show first that v, w can be chosen so that these paths are simple and vertex-disjoint. Say that P_1 and P_2 are not vertex-disjoint. Let $v_0 \in P_1$ be the first node along P_2 which is also in P_1. Then letting $v' = v_0$, we still have a path P_1' from T $\to v'$ and P_2' from $w \to v'$ since v' is in both paths, but now they are vertex-disjoint since all other shared vertices are further down P_2, and thus are no longer in P_2'. Likewise, say that P_2' and P_3 are not vertex-disjoint, and let w_0 be the first node along P_3 that they share. Then likewise, letting $w' = w_0$, we can construct vertex-disjoint paths P_3' from $w' \to$ B and P_2'' from $w' \to v'$ following the same procedure. Finally, if any of P_1', P_2'', and P_3 have self loops, we remove them. Concatenating these paths together in the undirected graph $\mathcal{G}_C$ yields an undirected path P from T — B, which is simple since the concatenated paths were simple and vertex-disjoint, so concatenation cannot add cycles. Create any spanning tree $\mathcal{T}$ for $\mathcal{G}_C$ that also contains P. Then $\mathcal{T}$ is a connected subgraph of $\mathcal{G}_C$ by construction, but since $\mathcal{T}$ is a tree, P must be the unique path from T $\to$ B. Then $\mathcal{G}_C$ is connected, but none of its undirected paths correspond to directed paths in $\mathcal{G}_\mathcal{P}$. $\square$

Thus, without path consistency, a controller which enforces that $\mathcal{G}_C$ remains connected may still control to a configuration in which no γ-strong path exists. Still, it is worth noting that, depending on the number of robots and the choice of edge weight function L_{ik}, controlling to such a configuration may not be feasible physically. Finally, we show that path consistency can be verified efficiently for a given $\mathcal{P}$. Thus, given a desired network team topology, one can determine whether it is viable before executing a mission.

Proposition IV.5. Given a path-induced subgraph $\mathcal{G}_\mathcal{P}$ path consistency can be verified in $O(|\mathcal{V}| + |\mathcal{E}|)$.

Proof. First, we can compute in $O(|\mathcal{V}| + |\mathcal{E}|)$ the set A of nodes reachable from T using BFS, and set a boolean array with indices $\{1, \dots, K, \mathrm{T}, \mathrm{B}\}$ to `True` iff its index is in A, requiring $O(|\mathcal{V}|)$. Then we can similarly find the set B of all nodes from which B can be reached by running BFS on the reversed graph. Finally, in $O(|\mathcal{V}| + |\mathcal{E}|)$, we find all nodes reachable from nodes in B along at least 1 edge using multi-source BFS, terminating if any such node is already set to `True`, which corresponds to such a path existing. $\square$

A natural symmetrized control graph for our purposes is that formed by a path from T to B of length $\lfloor K/(F+1) \rfloor$, since we can independently control $F+1$ such vertex-independent lines to enforce F-fault tolerance.

B. A Control Barrier Function For Safe Control

As stated above, our system evolves according to the dynamics

$$\dot{\mathbf{X}}(t) = \mathbf{A}V_\mathrm{T}(t) + \mathbf{B}\mathbf{u}(\mathbf{X}), \tag{7}$$

where $\mathbf{A} \triangleq \mathbf{e}_{2K+1}$ and $\mathbf{B} \triangleq \begin{bmatrix} \mathbf{1}_{2K} \\ \mathbf{0}_2 \end{bmatrix}$. We seek to define a safe controller $\mathbf{u}(\mathbf{X})$, such that the network with configuration $\mathbf{X}(t)$ has a γ-strong path from T $\to$ B for all $t \geq 0$. To do so, we take inspiration from the connectivity maintenance approach of [1], [28], [35] by defining a CBF which enforces that the algebraic connectivity of an undirected graph remain positive.

Recall that $\mathbf{W}_\gamma(\mathbf{X})$ denotes the weight matrix associated with configuration $\mathbf{X}$'s γ-threshold graph. We see that $\mathbf{W}_\gamma(\mathbf{X})$ is continuously-differentiable for all $\mathbf{X}$ except where $L_{ik}(\mathbf{X}) - \gamma = 0$. If our control graph is a tree then $\lambda_2 \geq \epsilon$ implies $L_{ik}(\mathbf{X}) - \gamma > 0$, but otherwise links can still be broken while maintaining connectivity. Thus, it is necessary to use a smooth approximation of the max operator to ensure a continuously differentiable CBF. In particular, consider the following *smooth max* function ([36], Lemmas 2.20-21):

$$M_s(x) = \begin{cases} 0 & x \leq 0 \\ \frac{xd(sx)}{d(sx)+d(1-sx)} & x > 0, \end{cases} \tag{8}$$

where $d(t) = e^{-\frac{1}{t}}$ if $t > 0$ and 0 otherwise, and $s > 0$ can be any positive number. It is simple to verify that $M_s(x)$ is nonnegative, continuously differentiable, and an underapproximation of the max function. Moreover, $\lim_{s\to\infty} M_s(x) = \max\{x, 0\}$ pointwise. Then we define *smoothed* weights $\mathbf{W}_\gamma^s(\mathbf{X})$ as follows:

$$\left[\mathbf{W}_\gamma^s(\mathbf{X})\right]_{ik} = M_s(L_{ik} - \gamma) \tag{9}$$

so that $\mathbf{W}_\gamma^s(\mathbf{X}) \leq \mathbf{W}_\gamma(\mathbf{X})$ entrywise. Then, given any symmetrized control graph $\mathcal{G}_C$, let $\mathbf{S} : \mathbb{R}^{(K+2)\times(K+2)} \to \mathbb{R}^{(K+2)\times(K+2)}$ denote the map from $\mathbf{W}_\gamma^s$ to the corresponding undirected communication matrix $\mathbf{W}_C$ of $\mathcal{G}_C$. That is, $\mathbf{S}(\mathbf{W}_\gamma^s) = \mathbf{W}_C$. Then we take our CBF to be the following:

$$h(\mathbf{X}) = \left(\lambda_2 \circ \mathbf{S} \circ \mathbf{W}_\gamma^s\right)(\mathbf{X}) - \epsilon, \tag{10}$$

for any $\epsilon > 0$, where $\lambda_2(\mathbf{W})$ is the Fiedler value of the graph laplacian $L \triangleq \mathrm{diag}\left\{\mathbf{1}^\top \mathbf{W}\right\} - \mathbf{W}$, which is continuously-differentiable when the Laplacian's eigenvalues are simple [30].

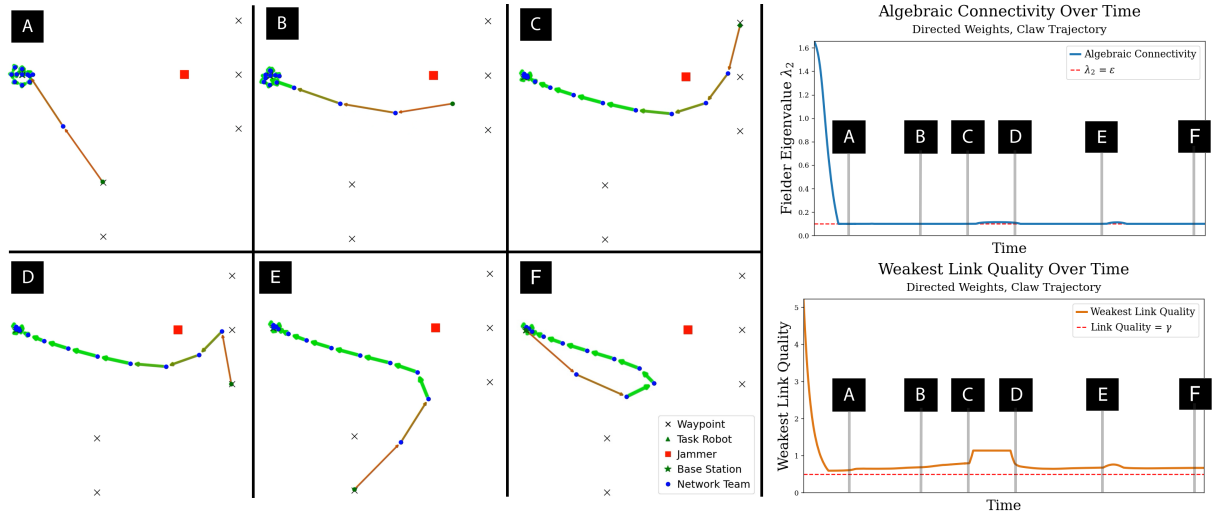

Fig. 3: **(Left)** Snapshots of a trajectory with controller (11)–(12) enforcing the connectivity of our symmetrized control graph. The task robot (T) moves through a series of waypoints. **(Top Right)** The Fiedler value of our symmetrized control graph over time. **(Bottom Right)** the link quality of the weakest link on the directed path from T to the base station —a γ-strong path exists if and only if this line remains above the dotted red line. Our controller maintains $\lambda_2 > \varepsilon$ throughout the trajectory, and consequently the directed path remains γ-strong throughout the mission duration.

Furthermore, note that $\mathbf{W}^s_\gamma(\mathbf{X})$ is continuously-differentiable and $\mathbf{S}$ is a linear map. Thus, h is continuously differentiable whenever the Laplacian has simple eigenvalues. Using this candidate CBF, we define our controller:

$$\mathbf{u}^*(\mathbf{X}) = \underset{\mathbf{u}\in\mathbb{R}^{K\times 2}}{\arg\min} \|\mathbf{u}\|_2^2 \tag{11}$$

$$\text{s.t.} \quad \frac{dh}{dt} \geq -\alpha(h(\mathbf{X})). \tag{12}$$

We verify below that this controller enforces the existence of a directed γ-strong path:

Theorem IV.6 (Set-Invariant Control)**.** If, for each $\mathbf{X}(t)$, (11)–(12) is strictly feasible and the Fiedler value λ_2 of the graph $(\mathbf{S} \circ W^s_\gamma)(\mathbf{X}(t))$ is simple (see Equation (10)), then its solution $\mathbf{u}^*(\mathbf{X}(t))$ is continuous, and this control ensures there exists a γ-strong path from T $\to$ B for all $t \geq 0$.

Proof. Notice that, since the Fiedler value is monotonic in each edge weight, $\left(\lambda_2 \circ \mathbf{S} \circ \mathbf{W}^\alpha_\gamma\right)(\mathbf{X}) \leq \left(\lambda_2 \circ \mathbf{S} \circ \mathbf{W}_\gamma\right)(\mathbf{X})$, and so if $h(x) > 0$, then $\left(\lambda_2 \circ \mathbf{S} \circ \mathbf{W}_\gamma\right)(\mathbf{X}) > 0$ as well. Then proof then follows directly from [37], noting that $\lambda_2 > 0$ is a sufficient condition for a γ-strong path to exist by Proposition IV.3. □

Since F-fault tolerance requires $(F+1)$ vertex-independent paths, and these paths only share nodes which cannot be controlled (that is, T and B), we can control to enforce F-fault tolerance by maintaining $(F+1)$ such CBFs on vertex-independent sets of paths $\mathcal{P}_1, \ldots, \mathcal{P}_{F+1}$.

V. Simulation Results

We verify our analytical results in simulation. We also compare our approach to the baseline [31], which we call the *minimum weight* controller. This controller also enforces connectivity using the CBF (11)–(12), but rather than using one of our symmetrized control graphs, it instead creates undirected weights using the minimum link quality in either direction. Our communication model (Equation (3)) uses hyperparameters $C_S = 2.75$, $C_J = 1$, $N_F = 0.1$, and $\delta = 0.01$. We set the minimum viable SINR to $\gamma = 0.5$, and set threshold $\epsilon = 0.1$ in our CBF (Equation (10)).

A. Claw Trajectory

We demonstrate the efficacy of our controller on a trajectory in which the task robot (T) follows a path of 6 waypoints (Figure 3). T begins to the left of the jammer, and can safely navigate above and to the right of the jammer before returning back to the base station. Plotting the algebraic connectivity confirms that our controller successfully enforces connectivity over time. The plot of the weakest link quality on the directed path to the base station ensures that a γ-strong path exists throughout the trajectory. The two 'bumps' occur when T moves towards its out-neighbor, improving that directed link's quality.

B. Comparison with Minimum Weight Controller

We compare the CBF controller (11)–(12) using our symmetrized control graph against the minimum weight controller [31]. Figure 4 shows these controllers following a *line trajectory* in which T passes directly over the jammer, and Figure 5 shows the Fiedler value and weakest directed link quality over time under each controller. At snapshot B, the reverse link from T has link quality 0, while its forward link is still above γ. Our controller continues to ensure that a γ-strong path exists, while the minimum weight CBF becomes infeasible, and as a result that controller fails. Thus, we see that our controller

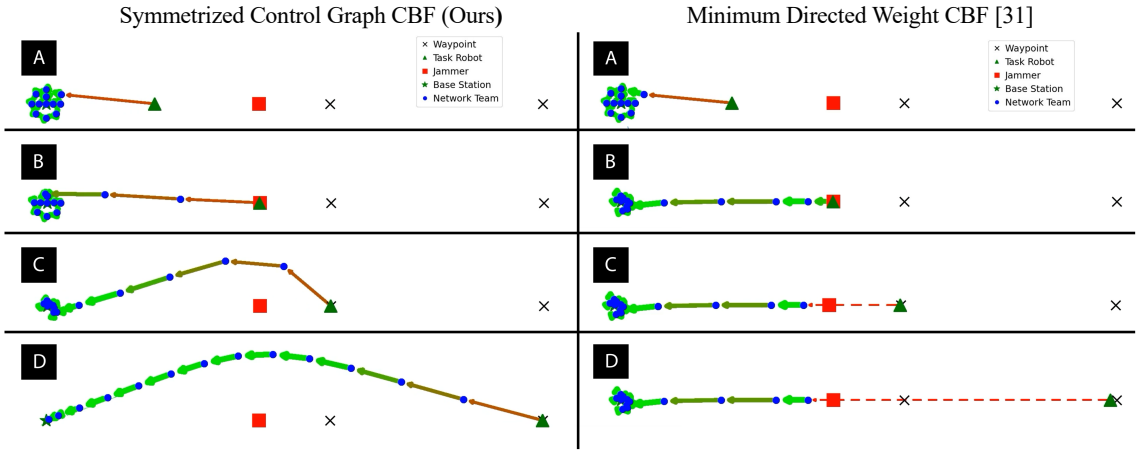

Fig. 4: Snapshots of a trajectory with controller (11)–(12), with the task robot moving in a straight line. **(Left)** Controlling using a symmetrized control graph, we see that a γ-strong path exists throughout the trajectory, with network team robots moving around the jammer to ensure that they can receive messages at rate γ. **(Right)** A trajectory generated by the minimum weight controller baseline [31] (see Section V). When the task robot passes over the jammer (snapshot B), the minimum weight CBF is infeasible, and the controller fails. When the task robot continues moving, the link quality eventually falls below γ (See Figure 5).

enables robust execution of more ambitious trajectories, and in particular those where T travels very close to the jammer.

VI. Discussion

Though this work is principally interested in asymmetric communication due to adversarial jamming, the graph-theoretic results of Section IV-A hold for any directed communication model. In particular, our symmetrized control graph approach generalizes in principle to environments with multiple jammers, which can be accommodated by adding additional interference terms to the link quality ((3)). However, adding additional jammers may increase the likelihood of infeasible trajectories.

For the single jammer case, the optimization (11)–(12) is infeasible for some trajectories, falling into two broad cases. First, if T ever moves too far from the base station, the K network team robots will become too far apart to transmit at rate γ, even in the absence of a jammer. Second, if the jammer power is high enough that two robots on opposite sides of the jammer cannot communicate at rate γ from any distance, then trajectories circumnavigating the jammer may yield configurations where task team members cannot safely cross from one side to the other without breaking their directed link. Finding tight conditions for the feasibility of the controller, and proactively routing the network team to anticipate link breaks, is left as a subject for future work.

In summary, we presented a novel approach for ensuring high-data rate directed communication in an autonomous robotic network in the presence of a jammer. Although out of scope for the current work, the formulation and results presented here provide a starting point for addressing more complex scenarios in the future, such as multiple jammers, moving jammers, or jammers with unknown position that can be learned and adapted to online.

References

[1] L. Sabattini, C. Secchi, N. Chopra, and A. Gasparri, "Distributed control of multirobot systems with global connectivity maintenance," *IEEE Transactions on Robotics*, vol. 29, no. 5, pp. 1326–1332, 2013.

[2] H. Sugiyama, T. Tsujioka, and M. Murata, "Integrated operations of multi-robot rescue system with ad hoc networking," in *2009 1st International Conference on Wireless Communication, Vehicular Technology, Information Theory and Aerospace Electronic Systems Technology*, 2009, pp. 535–539.

[3] C. Ghedini, C. H. Ribeiro, and L. Sabattini, "Toward efficient adaptive ad-hoc multi-robot network topologies," *Ad Hoc Networks*, vol. 74, pp. 57–70, 2018.

[4] K. M. Brian Lee, F. Kong, R. Cannizzaro, J. L. Palmer, D. Johnson, C. Yoo, and R. Fitch, "An upper confidence bound for simultaneous exploration and exploitation in heterogeneous multi-robot systems," in *2021 IEEE International Conference on Robotics and Automation (ICRA)*, 2021, pp. 8685–8691.

[5] C. Kanellakis, P. S. Karvelis, S. S. Mansouri, A.-A. Agha-Mohammadi, and G. Nikolakopoulos, "Towards autonomous aerial scouting using multi-rotors in subterranean tunnel navigation," *IEEE Access*, vol. 9, pp. 66 477–66 485, 2021.

[6] C. Robin and S. Lacroix, "Multi-robot target detection and tracking: Taxonomy and survey," *Autonomous Robots*, vol. 40, 08 2015.

[7] P. Zhu and W. Ren, "Multi-robot joint localization and target tracking with local sensing and communication," in *2019 American Control Conference (ACC)*, 2019, pp. 3261–3266.

[8] X. Huang, M. Sun, H. Zhou, and S. Liu, "A multi-robot coverage path planning algorithm for the environment with multiple land cover types," *IEEE Access*, vol. 8, pp. 198 101–198 117, 2020.

[9] A. Jamshidpey, W. Zhu, M. Wahby, M. Allwright, M. K. Heinrich, and M. Dorigo, "Multi-robot coverage using self-organized networks for central coordination," in *Swarm Intelligence*, M. Dorigo, T. Stützle, M. J. Blesa, C. Blum, H. Hamann, M. K. Heinrich, and V. Strobel, Eds. Cham: Springer International Publishing, 2020, pp. 216–228.

[10] M. Jurt, A. Aijaz, and Y. Jin, "Area coverage assessment and optimisation by mesh-connected mobile robots," in *2024 IEEE 35th International Symposium on Personal, Indoor and Mobile Radio Communications (PIMRC)*, 2024, pp. 1–5.

[11] J. Fink, A. Ribeiro, and V. Kumar, "Robust control for mobility and wireless communication in cyber–physical systems with application to robot teams," *Proceedings of the IEEE*, vol. 100, no. 1, pp. 164–178, 2011.

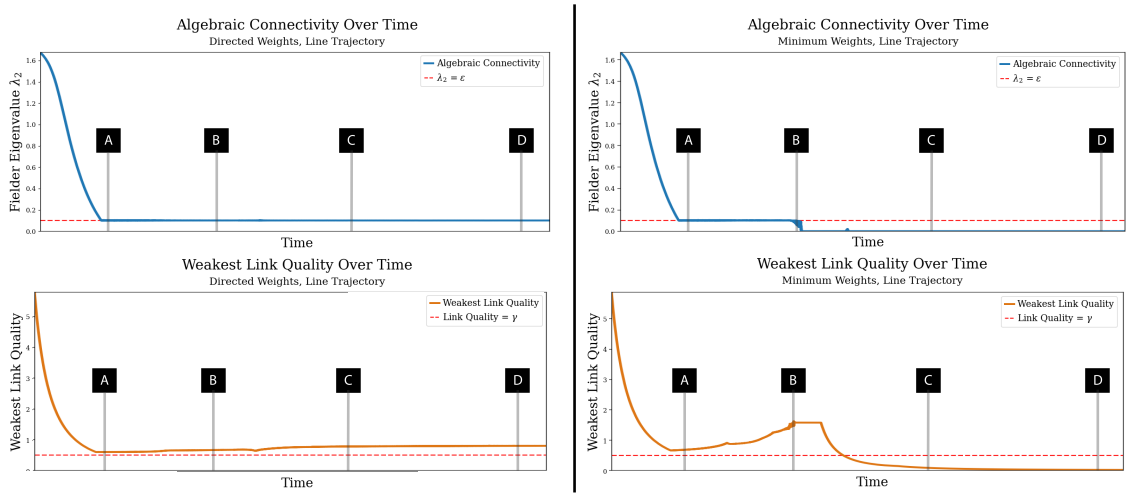

Fig. 5: **(Top)** The algebraic connectivity throughout the line trajectory in Figure 4. **(Left)** Network team controlled using our symmetrized control graph; and **(Right)** using the minimum weight controller baseline [31] (see Section V). **(Bottom)** The weakest link quality of the directed path from the task robot to the base station using each approach. Under our controller, a γ-strong path is maintained throughout the trajectory, indicated by the weakest link quality remaining above the dotted red line. The minimum weight controller CBF is infeasible at snapshot B, and so the controller breaks.

[12] ——, "Motion planning for robust wireless networking," in *2012 IEEE International Conference on Robotics and Automation*. IEEE, 2012, pp. 2419–2426.

[13] D. Mox, M. Calvo-Fullana, M. Gerasimenko, J. Fink, V. Kumar, and A. Ribeiro, "Mobile wireless network infrastructure on demand," in *2020 IEEE International Conference on Robotics and Automation (ICRA)*. IEEE, 2020, pp. 7726–7732.

[14] D. Mox, V. Kumar, and A. Ribeiro, "Learning connectivity-maximizing network configurations," *IEEE Robotics and Automation Letters*, vol. 7, no. 2, pp. 5552–5559, 2022.

[15] C. A. Balanis, *Antenna theory: analysis and design*. John wiley & sons, 2016.

[16] F. Causa and G. Fasano, "Multi-drone cooperation to improve navigation integrity in low altitude urban environments," in *2023 IEEE/ION Position, Location and Navigation Symposium (PLANS)*, 2023, pp. 34–45.

[17] J. de Curtò, I. de Zarzà, J.-C. Cano, and C. T. Calafate, "Enhancing communication security in drones using qrng in frequency hopping spread spectrum," *Future Internet*, vol. 16, no. 11, 2024. [Online]. Available: https://www.mdpi.com/1999-5903/16/11/412

[18] J. Zhou, W. Wang, and C. Zhang, "A gnss anti-jamming method in multi-uav cooperative system," *IEEE Transactions on Vehicular Technology*, pp. 1–14, 2025.

[19] C. Qu, R. Singh, A. E. Morel, F. B. Sorbelli, P. Calyam, and S. K. Das, "Obstacle-aware and energy-efficient multi-drone coordination and networking for disaster response," in *2021 17th International Conference on Network and Service Management (CNSM)*, 2021, pp. 446–454.

[20] W. Lee, J. Y. Lee, J. Lee, K. Kim, S. Yoo, S. Park, and H. Kim, "Ground control system based routing for reliable and efficient multi-drone control system," *Applied Sciences*, vol. 8, no. 11, 2018. [Online]. Available: https://www.mdpi.com/2076-3417/8/11/2027

[21] A. Hamdi, B. Alkouz, B. Shahzaad, A. Bouguettaya, A. G. Neiat, F. Salim, and D. Y. Kim, "Drone-as-a-service: Research challenges and directions," *Proceedings of the IEEE*, pp. 1–27, 2025.

[22] J. Diller, N. Dantam, J. Rogers, and Q. Han, "Communication jamming-aware robot path adaptation," in *2023 19th International Conference on Distributed Computing in Smart Systems and the Internet of Things (DCOSS-IoT)*. IEEE, 2023, pp. 768–773.

[23] M. M. Zavlanos and G. J. Pappas, "Potential fields for maintaining connectivity of mobile networks," *IEEE Transactions on robotics*, vol. 23, no. 4, pp. 812–816, 2007.

[24] P. Yang, R. A. Freeman, G. J. Gordon, K. M. Lynch, S. S. Srinivasa, and R. Sukthankar, "Decentralized estimation and control of graph connectivity for mobile sensor networks," *Automatica*, vol. 46, no. 2, pp. 390–396, 2010.

[25] M. Schuresko and J. Cortés, "Distributed motion constraints for algebraic connectivity of robotic networks," *Journal of Intelligent and Robotic Systems*, vol. 56, pp. 99–126, 2009.

[26] M. Ji and M. Egerstedt, "Distributed coordination control of multiagent systems while preserving connectedness," *IEEE Transactions on Robotics*, vol. 23, no. 4, pp. 693–703, 2007.

[27] A. D. Ames, S. Coogan, M. Egerstedt, G. Notomista, K. Sreenath, and P. Tabuada, "Control barrier functions: Theory and applications," in *2019 18th European control conference (ECC)*. Ieee, 2019, pp. 3420–3431.

[28] L. Sabattini, N. Chopra, and C. Secchi, "On decentralized connectivity maintenance for mobile robotic systems," in *2011 50th IEEE Conference on Decision and Control and European Control Conference*. IEEE, 2011, pp. 988–993.

[29] L. Wang, A. D. Ames, and M. Egerstedt, "Multi-objective compositions for collision-free connectivity maintenance in teams of mobile robots," in *2016 IEEE 55th Conference on Decision and Control (CDC)*. IEEE, 2016, pp. 2659–2664.

[30] M. Cavorsi, L. Sabattini, and S. Gil, "Multirobot adversarial resilience using control barrier functions," *IEEE Transactions on Robotics*, vol. 40, pp. 797–815, 2023.

[31] S. Bhattacharya and T. Başar, "Graph-theoretic approach for connectivity maintenance in mobile networks in the presence of a jammer," in *49th IEEE Conference on Decision and Control (CDC)*. IEEE, 2010, pp. 3560–3565.

[32] S. Bhattacharya, "On the construction of barrier in a connectivity maintenance game," in *2013 European Control Conference (ECC)*. IEEE, 2013, pp. 3338–3345.

[33] D. Halperin, W. Hu, A. Sheth, and D. Wetherall, "Predictable 802.11 packet delivery from wireless channel measurements," *ACM SIGCOMM computer communication review*, vol. 40, no. 4, pp. 159–170, 2010.

[34] R. Diestel, *Graph theory*. Springer Nature, 2025, vol. 173.

[35] B. Capelli and L. Sabattini, "Connectivity maintenance: Global and optimized approach through control barrier functions," in *2020 IEEE International Conference on Robotics and Automation (ICRA)*. IEEE, 2020, pp. 5590–5596.

[36] J. M. Lee, "Smooth manifolds," in *Introduction to smooth manifolds*. Springer, 2003, pp. 1–29.

[37] P. Ong, B. Capelli, L. Sabattini, and J. Cortés, "Nonsmooth control barrier function design of continuous constraints for network connectivity maintenance," *Automatica*, vol. 156, p. 111209, 2023.